Two-Body Abrasive Wear Behavior of Particulate Filled Polyamide66/Polypropylene Nanocomposites

B. Suresha,[1] B. N. Ravi Kumar[2]

[1]*Department of Mechanical Engineering, The National Institute of Engineering, Mysore 570008, Karnataka, India*
[2]*Department of Mechanical Engineering, Bangalore Institute of Technology, Bangalore 560004, Karnataka, India*

Received 21 December 2009; accepted 26 May 2010
DOI 10.1002/app.32909
Published online 30 August 2010 in Wiley Online Library (wileyonlinelibrary.com).

ABSTRACT: An experimental characterization of the abrasive wear behavior of clay and clay plus short carbon fiber filled polyamide66/polypropylene (PA66/PP) nanocomposites has been investigated. Two-body abrasive wear studies were carried out using pin-on-disc wear tester under multi-pass condition against the water proof silicon carbide abrasive paper. It was observed that the clay reinforcement is detrimental to the abrasive wear resistance of PA66/PP blend. A combination of clay and short carbon fiber in PA66/PP blend improved the abrasive wear performance than those of clay filled PA66/PP nanocomposites. Further, on the basis of microscopic observation of the worn surfaces, dominant wear mechanisms were discussed. © 2010 Wiley Periodicals, Inc. J Appl Polym Sci 119: 2292–2301, 2011

Key words: nanocomposites; blending; hardness; two-body abrasion; scanning electron microscopy

INTRODUCTION

In recent years, polymer is extensively utilized in tribological components such as cams, brakes, bearings, and gears because of their self-lubrication properties, lower friction, and better wear resistance. The inherent weakness of polymers could be improved successfully by using various special fillers (micro to nano sized particles); more and more polymer composites are now being used as sliding components, which were formerly composed of metallic materials only. Nevertheless, new developments are still under way to explore other fields of application for these materials and to tailor their properties for extreme loading and environmental temperature conditions. The current global nanocomposite market size is around US$ 300 million and is expected to exceed US$ 1 billion within the next five years.[1,2] Currently, clay filled nanocomposites account for almost 25% by volume of total nanocomposites usage and their market share is rapidly increasing.

Abrasive wear is the most important among all the forms of wear because it contributes almost 63% of the total cost of wear.[3] In two-body abrasion, wear is caused either by hard protuberances on one surface which can only slide over the other.[4] Abrasive wear situations are encountered in applications such as vanes and gears; pumps handling industrial fluids; bearings in steel mills subjected to heat; chute liners abraded by coke, coal, and mineral ores; food processors etc.[5]

The modification of mechanical and tribological behavior of filler and/fiber reinforced polymer composites has been reported[5–12] to be quite encouraging. Most studies on the influence of filler material, in the case of polymer composites sliding against metallic counter faces have reported on the reduction of wear rate and coefficient of friction. In addition to the higher mechanical strength obtained due to the addition of fillers in polymer composites, there is direct cost reduction due to the less consumption of matrix material. The wear was considerably reduced with the addition of CuO and CuS to polytetrafluoroethylene (PTFE), CuS, CuF_2, CaO, PbS, and AgS to polyamide11, nanoclay, graphite, short carbon fiber and nanoclay to polyamide66 and CuO, CuS, and CuF_2, to polyetheretherketone (PEEK).[6–11] The wear rate is increased when the fillers such as BaF_2, CaF_2, ZnF_2, SnF_2, ZnS, SnS, ZnO, and SnO were added to some polymers.[9,12] The mechanism of filler action in reducing the wear rate of polymers has recently been a subject of intense study. Considerable attention has thus been paid in the last 30 years to study the tribological properties of polymer composites. Reviews of such works may be found in articles by Briscoe and Tweedale,[13] Sinha and Biswas,[14] Zum Gahr,[15] Friedrich et al.,[16] Bijwe et al.,[17] and Suresha et al.[18] Some of the fillers

Correspondence to: B. Suresha (sureshab2004@yahoo.co.in).

© 2010 Wiley Periodicals, Inc.

that are effective in reducing friction and wear are MoS_2, CuO, CuS, graphite, and Al_2O_3.

Inorganic particles are well known to enhance the mechanical and tribological properties of polymers, and this issue has been widely investigated in the past decades. It has been found that the friction and wear properties varied continuously with the compositions for most polymer blends and particle size plays an important role in the improvement of wear resistance. Optimal properties were found at a certain composition, although some data reported were contradicting.[19–23] Incorporation of fibers and fillers in polymers affects the tribo performance, but it is found to be beneficial under some wear conditions while detrimental in some other wear situations.[24–26]

Many researchers have studied two-body wear behavior of polymers in general and polymer composites in particular.[27–30] Ozel[29] studied the abrasive wear of glass fiber reinforced polymer polyamide46 (PA46) and polyphenylenesulfide (PPS) composites and found that the wear rate was considerably reduced with the reinforcement of glass fibers in PA46. Unal and Findik[30] indicated that the specific wear rate of PA46 + 30% glass fiber and PA66 against PPS + 30%glass fiber reinforced polymer composite counterpart are about in the order f 10^{-13} m^3/Nm. They concluded that from point of tribological performance, PA46 + 30% glass fiber is a more suitable engineering thermoplastic composite material for electrical contact breaking applications. To improve the wear resistance, various kinds of micrometer sized particles, e.g., TiO_2, ZrO_2, SiC, and copper compounds were incorporated into different polymers matrices, e.g., polyetheretherketone (PEEK), polyamide (PA), polyphenylene sulfide (PPS), polytetrafluoroethylene (PTFE) polypropylene (PP), and polystyrene (PS).[7,6,31–35] The improvements of the wear resistance were due to either mechanical or chemical reasons. Wang et al.[36] studied the mechanical and tribological behavior of the blend of PA66/UHMWPE with MAH-g-HDPE as compatibilizer. The results showed that the addition of UHMWPE reduced the wear rate.

In filled polymer composites, the particle size plays an important role in the improvement of wear resistance. Reducing the particle size to a nano-scale level is assumed to improve significantly the composite efficiency; nano particles filled polymers, the so-called polymer nanocomposites, are very promising materials for various applications. They are expected to replace polymers, polymer blends and their traditional composites in parts produced by melt processing techniques. Recent investigations on the tribological behavior of organoclay filled polyamide6 (PA6) by Srinath and Gnanamoorthy[37] and Dasari et al.[38] show a low friction and high wear resistance since the size of nano additives is of the order of surrounding polymer chains and increases bonding of particle to the polymer matrix. Also, the nanosized filler tends to produce a tenacious transfer layer on the counterface, which protects the composite surface from direct contact with the counterface thereby reducing the friction and wear of nanocomposites. The addition of nanoclays to form a polymer nanocomposite is another means to modify the properties of material. The addition of 2–5% by weight of exfoliated clays can lead to improvements in thermal and mechanical properties in comparison to the unfilled polymer.[39–41] The montmorillonite (MMT) as filler in thermoplastic polymers has already been a matter of study.[42–47]

Blending of PA6 with PP leads to materials with improved chemical and moisture resistance, dimensional stability, and reduced cost. However, to achieve these advantages, some form of compatibilization is generally required.[48,49] In the case of PA6/PP/PPgMAH blends, succinic anhydride groups on PP grafted with maleic anhydride (PPgMAH) are able to react with PA6 amine terminal groups competitively to form PA6 grafted PP (PA6gPP) copolymer during melt processing.[49] However, the major drawback of PA6/PP blends is their low impact strength, particularly at low temperatures. According to the author's knowledge, no study is available in the literature on two-body abrasive wear behavior of PA66/PP blends and their nanocomposites.

In view of the above, it was thought that because of nano-sized particulate filler in PA66/PP composite, the material should have improved the wear resistance. An investigation was therefore undertaken to study the two-body abrasive wear behavior of nanoclay filled and short carbon fiber plus nanoclay-filled PA66/PP composites and compared with that of PA66/PP blend. The effects of grit size, load and abrading distance on the wear volume, specific wear rates, and dominant wear mechanisms have been discussed.

EXPERIMENTAL DETAILS

Materials used

Polymer alloy of polyamide66 and polypropylene and particulates namely nanoclay (NC) and short carbon fiber (SCF) filled PA66/PP composites were prepared for this study with compatibilizer. The polymer alloy produced consists of 50% by weight of each component. Maleic anhydride polypropylene (MAgPP) as compatibilizing agent was used in this study. The amount of compatibilizer added was 1 wt % based on previous literature and this

TABLE I
Data on Polymer, Particulates, and Compatibilizing Agent

Samples	Tensile strength (σ) MPa	Strain (*e*) (%)	Hardness (Shore-D)	Density (g/cm^3)	Factor (σ *e*)
PA66/PP	30.65	0.13	64	0.9072	3.985
NC-PA66/PP	22.20	0.08	71	1.0282	1.776
SCF+NC-PA66/PP	49	0.07	75	1.0785	3.34

compatibilizer proportion was high enough for interaction with PA66/PP interface. The sources and characteristics of these materials are listed in Table I.

Compounding

Before compounding, the PA66 and PP granules and fillers were dried at 80°C for 10 h in an air circulated oven and then dry mixed with polyamide66 and other additives. Composition shown in Table I was mixed and extrudated in a corotating twin extruder (Segmented Barrel and Segmented screw type). The barrel length to diameter (*L/D*) ratio of the screw is 40 : 1. Mixing speed of 60 rpm was maintained for all the compositions. The extrudates from the die were quenched in a tank at 20–30°C and then palletized. For the melt blending the temperatures from the feed zone to the die of the extruder were 205, 235, 245, 255, and 265°C respectively. The extrudates of the composition was palletized in palletizing machine. The rpm of the pelletizer was maintained at 70 rpm.

Injection molding

The granules of the extrudates were pre dried in an air circulated oven at 80°C for 10 h and injection molded in a microprocessor based injection molding machine (75 Tonnage Screw Type: Hydraulic Horizontal Injection Molding machine) fitted with a master mold containing the cavity for tensile strength, flexural, and impact specimens. After its ejection from the mold, specimens were cooled in ice-water. Processing parameters for the injection molding, the temperatures of the barrel were kept at 200, 235, and 260°C, respectively. The details of the composites fabricated for the present investigation are given in Table II.

Density and hardness measurement

Densities of the composites were determined using a high precision electronic balance (Mettler Toledo machine Model AX 205) following the Archimedes principle. Shore hardness of the samples was measured as per ASTM D2240, by using a Hiroshima make Hardness Tester (Durometer).

X-ray diffraction

The interlayer distance of nanoclay in the nanocomposites was studied by wide angle X-ray diffraction (XRD). Both for the nanoclay and the nanocomposites, XRD was recorded using X-ray diffractometer (RIGHKU-Make), Copper K_α target is used. The basal spacing reflection of samples was calculated from Bragg's equation by monitoring the diffraction angle 2θ from 2–10° at scanning rate of 0.5° min^{-1}.

Abrasive wear test

Two-body abrasive wear tests were performed using a single pin-on-disc wear testing machine as shown in Figure 1. Test samples were prepared after proper cutting and polishing to 8 mm × 8 mm × 2 mm size. The composite sample was abraded against the water proof silicon carbide (SiC) abrasive papers of 320 and 600 grit sizes at a constant running speed of 382 rpm in multipass condition (Fig. 2).

Scanning electron microscopy

Scanning electron microscope (SEM) of SiC abrasive papers having grit size 320 and 600, before wear test are shown in Figure 3(a,b), respectively. The

TABLE II
Composites Fabricated for This Study

Polymer/filler	Designation	Grade	Melting point (°C)	Density (g/cm^3)	Source
Polyamide66	PA66	Zytel 101L NC010	263	1.14	DuPont Co.Ltd
Polypropylene	PP	MI 3530	168	0.90	IPCL, India.
Maleic anhydride polypropylene	MAgPP	Fusbond	133	0.96	DuPont Co.Ltd
Nanoclay	NC	Nanomer	–	2.35	Sigma-Aldrich Inc.
Short carbon fiber	SCF	PAN based T300	–	1.74	Fibraplex Corp Celina TN

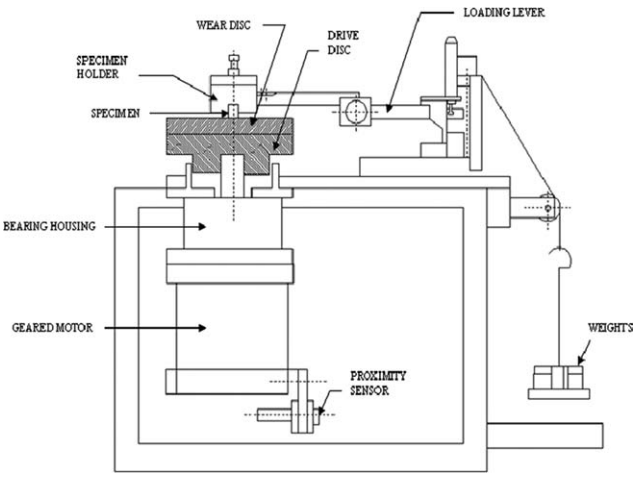

Figure 1 Schematic of pin-on-disc wear setup.

embedded hard SiC particles abrade the test samples. A constant sliding velocity of 2 m/s and two loads of 5 and 10 N were applied. The weight loss measurements were carried out for different abrading distances namely 50, 100, 150, and 200 m. Before and after wear testing, samples were cleaned with brush to remove wear debris. The wear was measured by the loss in weight (Mettler TOLEDO; 0.1 mg accuracy), which was then converted into wear volume using the measured density data. The specific wear rate (K_s) was calculated from the following equation:

$$K_s = \frac{\Delta V}{L \times d} \quad (1)$$

where ΔV is the volume loss in m^3, L is the load in Newton's, and d is the abrading distance in meters. After wear test, the worn surfaces of specimens were examined using a scanning electron microscope (JSM 840A model of JEOL make). Before the examinations, a thin gold film was coated on the worn surface by sputtering to achieve a conducting layer.

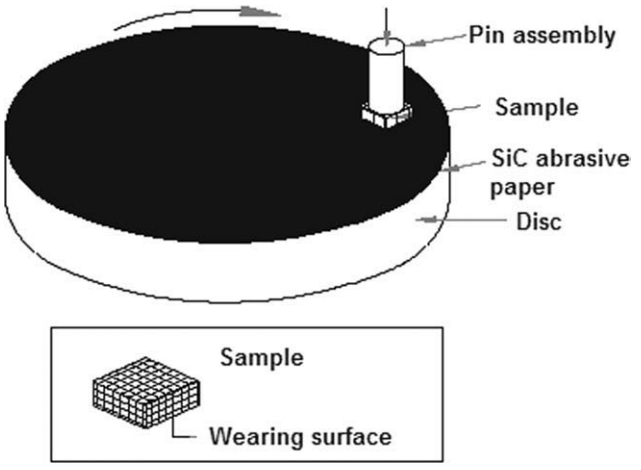

Figure 2 SiC paper fixed on rotating disc and composite sample glued to a pin.

RESULTS AND DISCUSSION

X-ray diffraction

Figure 4 shows the XRD pattern in the range of $2\theta = 2$–10° for nanoclay and PA66/PP nanocomposites. The XRD pattern of the nanoclay shows a broad intense peak at around $2\theta = 4.2^\circ$ corresponding a basal spacing 21.03 Å (By using Bragg's law $2d \sin \theta = n\lambda$, where λ is the X-ray wave length (1.54 Å), $2\theta = 4.2^\circ$). The XRD pattern of PA66/PP, nanoclay-filled PA66/PP, graphite filled PA66/PP composites do not show a characteristics basal reflection of the nanoclay. However they show shoulder at $2\theta = 2^\circ$. This is a clear indication that portion of nanoclay is only intercalated. Chow et al.[48] and Wahit et al.[50] have reported a similar observation in the case of polyamide/polypropylene nanocomposites. The absence of the characteristic clay d_{001} peak indicates the exfoliation of the clay platelets in the PA66/PP matrix.

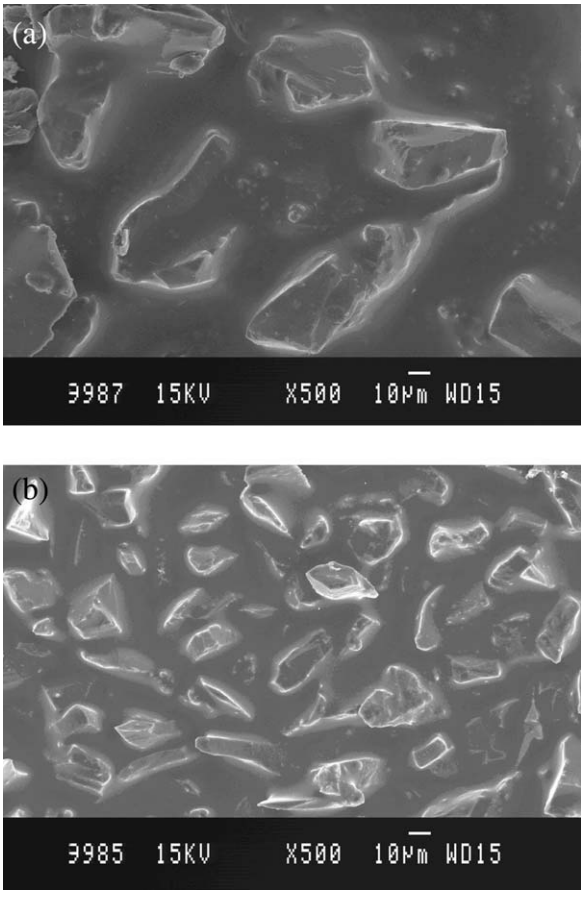

Figure 3 Scanning electron micrographs of SiC paper before wear test: (a) 320 grit and (b) 600 grit.

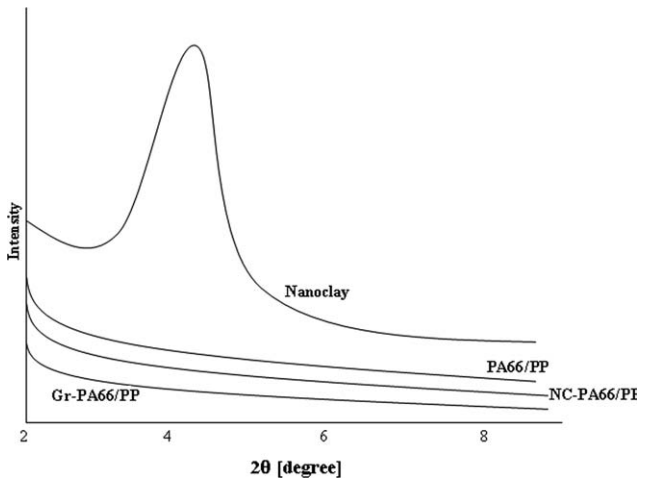

Figure 4 XRD spectra for the nanoclay and PA66/PP nanocomposites.

Abrasive wear volume and specific wear rate

The variation in abrasive wear volume as a function of abrading distance of PA66/PP, NC-PA66/PP, and SCF+NC-PA66/PP blends is presented in Figures 5(a,b) and 6(a,b) for different grit size of the SiC paper. A test conducted using coarse grit 320 having an average particle size 46.2 μm, resulted in higher wear volume loss in all the samples tested. Further, excessive wear was exhibited by the particulate filled PA66/PP composites. The abrasive wear performance of samples on grit 320 is poor due to the large sized abrasive particle, which removes more material during the abrasion process (Fig. 5). The material removal rate is high owing to the plowing and cutting action of the coarse grits. The wear volume data of all samples revealed that the wear volume tends to increase almost linearly with increasing abrading distance and strongly depends on both applied normal load and the grit size of abrasive paper. Figure 5(a,b) show that the wear volume loss of NC-PA66/PP is greatly increased with increase in abrading distance against 320 grit SiC paper. Increase in normal load increases the contact stresses, depth of penetration of the grit on the sample surface and hence the wear volume loss. On the 600 grit abrasive paper (average particle size of 26 μm), the difference between the specific wear rates of the composites are smaller compared with 320 grit abrasive paper as shown in Figure 6.

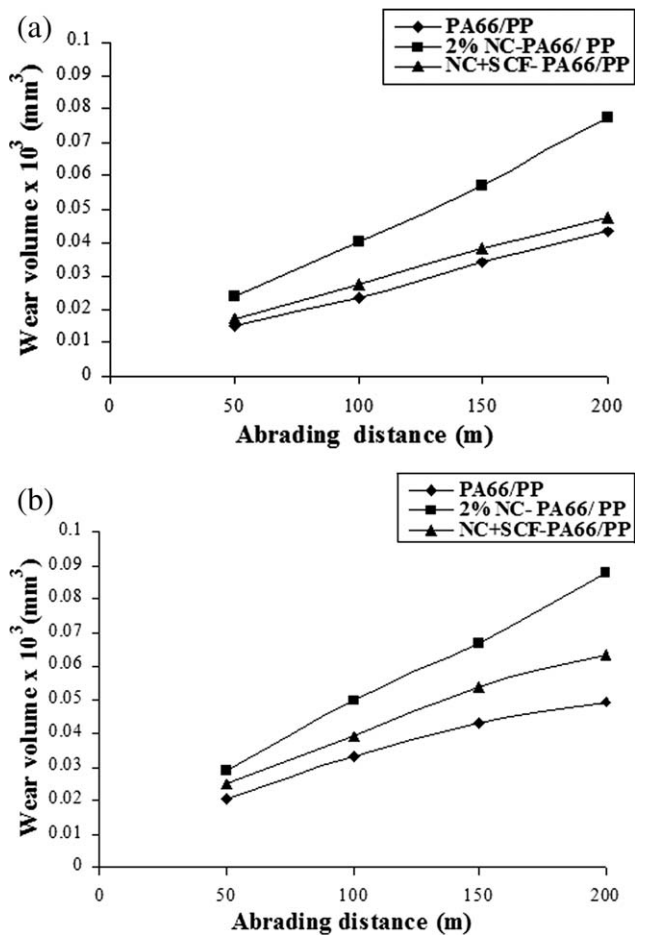

Figure 5 Effect of abrading distance on the wear volume loss of unfilled and filled PA66/PP blends against 320 grit SiC paper: (a) 5 N and (b) 10 N.

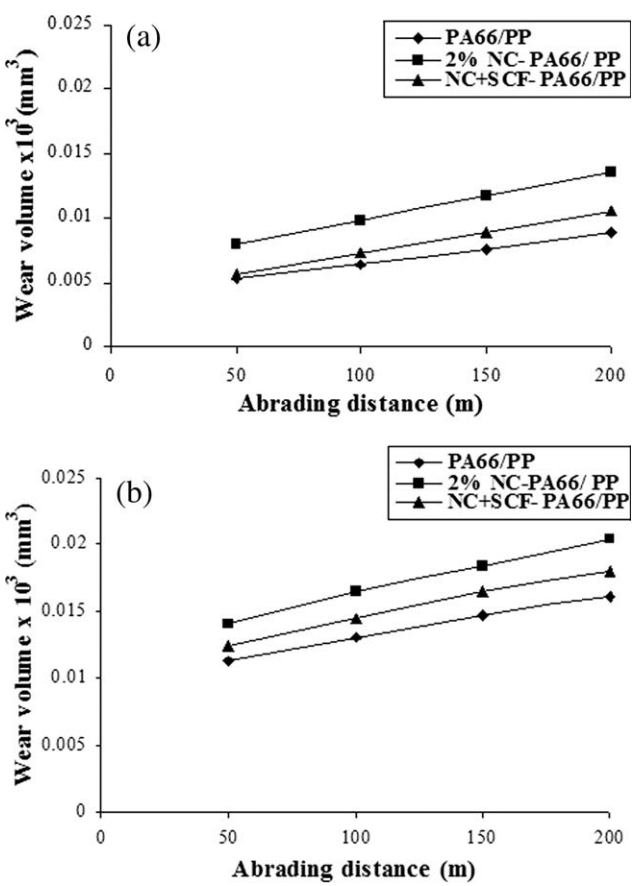

Figure 6 Effect of abrading distance on the wear volume loss of unfilled and filled PA66/PP blends against 600 girt: (a) 5 N and (b) 10 N.

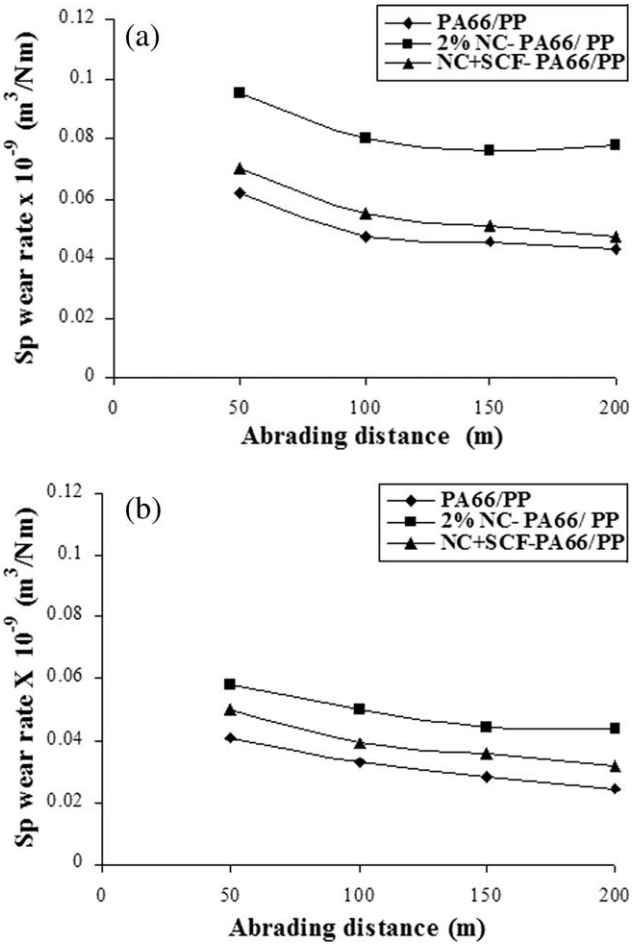

Figure 7 Effect of abrading distance on the specific wear rate of unfilled and filled PA66/PP blends against 320 girt: (a) 5 N and (b) 10 N.

Additions of short carbon fiber affect the abrasive wear of the blend composites. Under 5 and 10 N loads, SCF+NC-PA66/PP showed a lower abrasive wear volume loss than that of NC-PA66/PP.

The variation in the specific wear rate with increase in abrading distance slid against 320 grit and 600 grit abrasive papers is shown in Figures 7(a,b) and 8(a,b), respectively. The specific wear rate decreases with increasing abrading distance, load, and grit size of the abrasive paper for all samples tested. Figure 7(a,b) show the specific wear rate of samples abraded against 320 grit SiC paper. It can be seen that the specific wear rate is in the range 0.07761×10^{-9} to 0.04343×10^{-9} m^3/N m against 320 girt at 5 N applied load for SCF+NC-PA66/PP composite. For the same sample under same test conditions, the specific wear rate is much less and lies in the range 0.02262×10^{-9} to 0.01057×10^{-9} m^3/N m against 600 grit SiC paper.

The specific wear rate data of the materials under multipass two-body abrasive wear reveals that it tends to decrease with increasing abrading distance, load, and decreases with increase in grit of SiC. Higher specific wear rate was noticed for NC-PA66/PP compared to SCF+NC-PA66/PP composite. The wear resistance is better in short carbon fiber reinforced NC-PA66/PP nanocomposite and it can be attributed to inherent better mechanical properties and self lubricating nature of graphite. The chemical interaction between the graphite particles and the MAgPP compatibilized PA66/PP blend leading to better adhesion because of greater polymer-filler interaction. Also, NC-PA66/PP nanocomposites with SCF reinforcement, improved the mechanical properties such as specific stiffness, specific strength, excellent resistance to corrosion, and fatigue performance and in turn results in improved wear behavior. Figures 7 and 8 clearly illustrate the effect of filler components (nanoclay and SCF) on the specific wear rate of composites under different test conditions. In addition the Figures 6 and 7 indicate that the unfilled PA66/PP exhibits the lowest wear rate under all test conditions. The ranking of tested samples from lowest to highest were as follows: PA66/PP < SCF+NC-PA66/PP < NC-PA66/PP.

The influence of fiber and/or fillers on the abrasive wear resistance of neat polymer is a more complex and unpredictable phenomenon.[51] Lancaster[52]

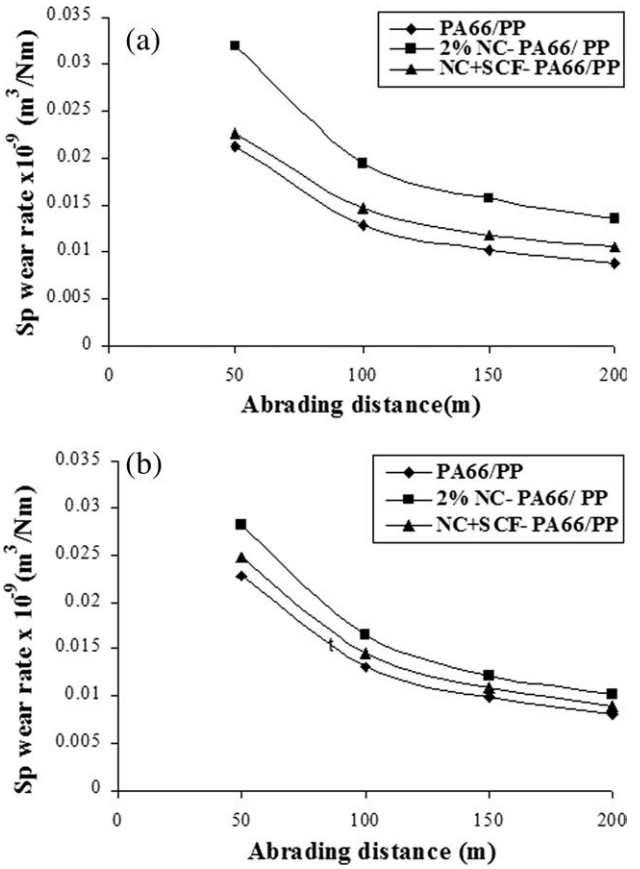

Figure 8 Effect of abrading distance on the specific wear rate of unfilled and filled PA66/PP blends against 600 girt: (a) 5 N and (b) 10 N.

TABLE III
Mechanical Properties Particulate Filled PA66/PP Composites.[11]

Material designation	Composition by wt %		
	Polypropylene (PP)	Polyamide66 (PA66)	Particulate filler
PA66/PP	50	50	–
NC-PA66/PP	48	50	2(nanoclay)
SCF+NC-PA66/PP	38	50	10+2 (SCF+NC)

studied abrasive wear resistance of thirteen polymers reinforced with 30% short carbon fiber and reported that wear resistance is improved for seven polymers while for six polymers it is deteriorated. Friedrich[27] reported that abrasive wear resistance of a thermoplastic will not improve by reinforcing with short fibers if the wear mechanism is highly abrasive in nature. The purpose of particulate filler inclusion into polymers is to improve their mechanical properties, but the effects on wear are not always beneficial.

Various efforts have been made to correlate abrasive wear to appropriate mechanical of other physical properties.[53,54] According to Lancaster[53] the σe factor (where σ is the ultimate tensile strength and e is the elongation at break) is of more importance. Although the addition of fillers and reinforcements increase the strength and stiffness of the polymers, there is generally a corresponding decrease in elongation at break. The product σe for a reinforced polymer may thus become smaller than that for a neat polymer, with a consequent reduction in abrasive wear resistance. The model proposed by Ratner and Farberova[54] states that the rate of material removal is inversely proportional to the product of stress and stain at rupture. They consider that reduction in elongation at break is the key factor influencing the abrasive wear resistance of filled polymer composites. Mechanical properties of the PA66/PP based nanocomposites were listed in Table III.[11] In this work for the composites tested, the wear resistance increased with increase in σe factor (Table III) and the experimental results are in good agreement with the reported literature.[3,53,54]

Worn surface morphology

Scanning electron photomicrographs of worn surfaces of samples are shown in Figures 9–11. Several mechanisms have been proposed to explain how material is removed from the surface during abrasion. Because of the complexity of abrasion, no one mechanism completely contributes to all the wear loss. In general, the abrasive wear process involves four different mechanisms namely microcutting, microploughing, microfatigue, and microcracking.[46] Using SEM photomicrographs it is possible to identify qualitatively the dominant wear mechanisms under abrasion.

Figure 9(a,b) shows worn surface of PA66/PP blend abraded against 320 and 600 grit SiC abrasive papers, respectively. It can be seen that the wide and deep grooves were paralleled along the friction direction on the wear surface of the PA66/PP blend. Splitting can also be seen. Obviously, the wear

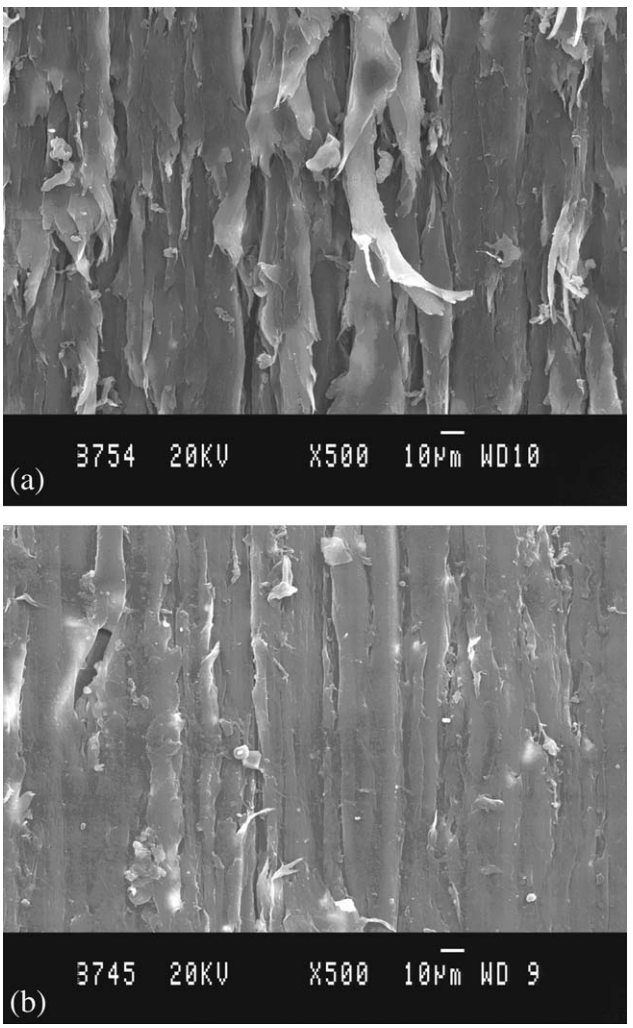

Figure 9 Worn surfaces of PA66/PP blends at 10 N and 200 m: (a) 320 grit and (b) 600 grit.

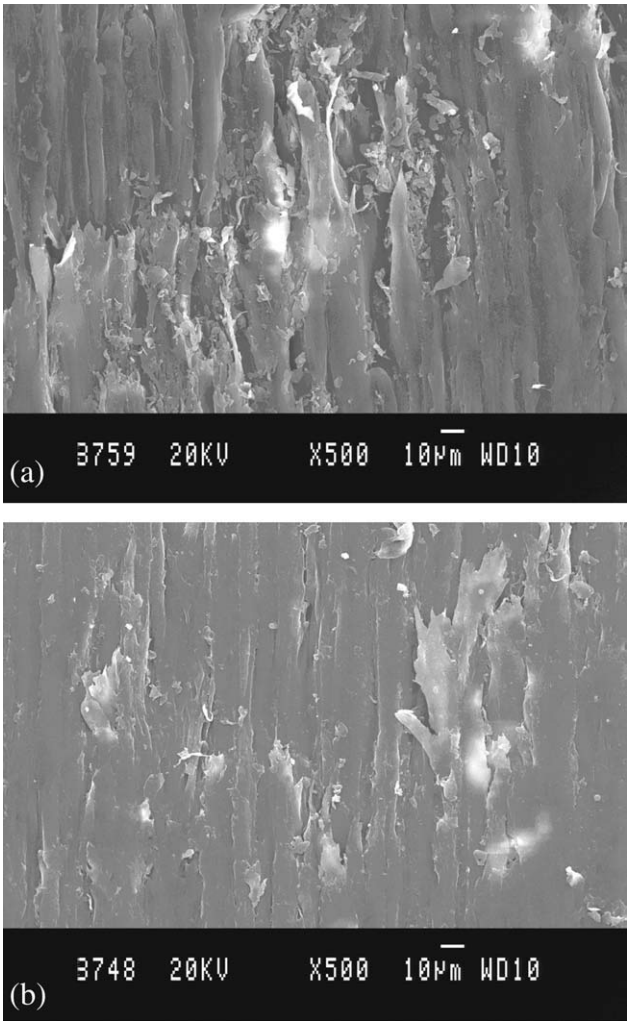

Figure 10 Worn surfaces of NC-PA66/PP nanocomposite at 10 N and 200 m: (a) 320 grit and (b) 600 grit.

mechanism of PA66/PP blend was microcutting. In the sample slid against a very rough abrasive paper (grit 320), the individual grains penetrate deeply into the surface of the material, subsequently removing material from the surface by an extensive microcutting process. During this process, the polymer matrix is highly plastically deformed before being separated owing to additional microploughing so that less wear debris is formed. It is noticeable that furrows and long tendrils are present on the worn surface. Surfaces with wavy stick-slip marks show regular deformation without large material removal. However, the worn surface of the same sample abraded against 600 grit showed less damage to the surface and narrow grooves due to very fine size of the abrasive particles. Further, the worn surface is relatively smooth and peeling of PP and PA66 are constrained due to that the PA66 effectively support the load from the 600 grit SiC paper.

Addition of clay affects the abrasive wear mechanism. SEM pictures of the worn surface of clay-filled PA66/PP nanocomposites whose clay content was 2 wt % are shown in Figure 10(a,b). In Figure 10, the grooves became narrow and shallow, and the splitting became weak as compared with Figure 9. From Figure 10(a,b), it can be seen that in the both cases of abrasive grit size of 320 and 600, there exist more wear debris on the worn surfaces, leading to deteriorating the wear resistance. Further, it is noticeable that long smooth plowed furrows are present and long tendrils are absent on the surface, which indicate that the clay-filled nanocomposite behave in a predominantly cutting manner and most material is cut and detached from the surface and some being displaced. As polyamide is ductile, the material removal by plowing mechanism is dominant.[47] Inclusion of clay in PA66/PP nanocomposite becomes brittle and cutting action is more predominant On the worn surface of blended composite abraded against 320 grit SiC paper, the abrasive grooves are narrow and wider [Fig. 10(a)]. However, the worn surface of the same sample slid against 600 grit SiC

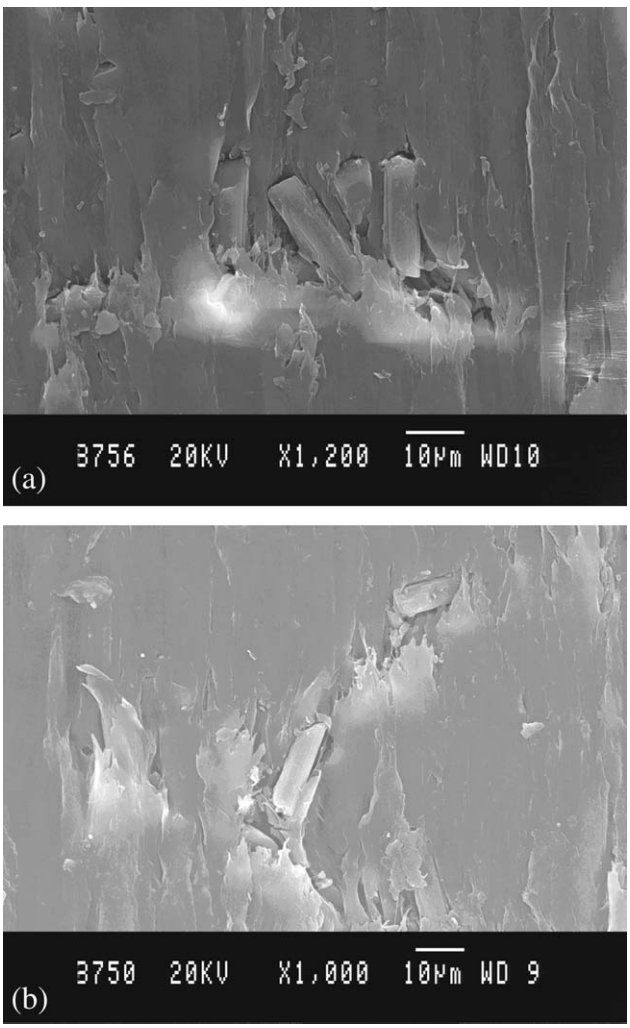

Figure 11 Worn surfaces of NC+SCF-PA66/PP nanocomposite at10 N and 200 m: (a) 320 grit and (b) 600 grit.

paper indicate shallow and no grooves due to the smaller size of the abrasive particles [Fig. 10(b)]. Comparing the photomicrographs of the composites tested, the extent of damage is more in case of NC-PA66/PP composite [Fig. 9(a,b)].

Figure 10 shows the photomicrographs of the NC+SCF-PA66/PP composite. Figure 10(a,b) exhibit the worn surfaces slid against SiC paper having grit size of 320 and 600, respectively. From Figure 11(a,b), it can be seen that in the both cases of abrasive grit size of 320 and 600, there exist less wear debris on the worn surfaces, leading to improved wear resistance. On the worn surface of nanocomposite abraded against 320 grit SiC paper, the abrasive grooves are not seen and the surface is relatively smooth the peeling of matrices are constrained [Fig. 11(a)]. However, the worn surface of the same sample slid against 600 grit SiC paper indicate shallow and no grooves due to the smaller size of the abrasive particles [Fig. 11(b)]. Further, from Figure 11, the wear of the surface became severe again, quite a few pits of fatigue flaking and few fibers bent could be seen. This indicates that the wear mechanism of NC+SCF-PA66/PP nanocomposite was fatigue wear and abrasive wear. In the meantime, it can be inferred from the above that the morphologies of the worn surface were relevant to the wear loss of the composites. Comparing the photomicrographs of the composites tested, the worn surface of SCF+NC-PA66/PP is relatively smooth, less damage to the matrix when compared to clay-filled PA66/PP composite.

CONCLUSIONS

Under in influence of grit size of abrasive the wear of PA66/PP blend increases when the blend is filled with clay and short carbon fiber. Further effects of load and abrading distance on the abrasive wear behavior the following observations and conclusions could be made.

- Abrasive wear of PA66/PP and their nanocomposites strongly depends on the experimental test parameters such as load, grit size and abrading distance.
- Nanoclay plus short carbon fiber filled PA66/PP showed better wear resistance than the nanoclay-filled PA66/PP composite. The difference in the abrasive wear behavior of particulate filled composites was more pronounced against 320 grit SiC paper.
- The abrading distance, load, and abrasive grain size influences the abrasion volume loss as well as specific wear rate.
- Fairly better correlations between the wear volume and selected mechanical properties were obtained for unfilled and filled PA66/PP nanocomposites.
- Microcutting and microploughing are the dominant wear mechanisms characterized by the formation of deep grooves with extruded filaments of matrix at the edges of the grooves.

The authors thank N. Govinda Raju, Chief Executive Officer, Magnum Engineers, Bangalore, for providing the testing facilities. The authors are thankful to the Management and Principal Dr. M.S. Shiva Kumar, The National Institute of Engineering, Mysore, India, for their encouragement. The authors are also thankful to M. Ganesh, Managing Director, GLS Polymers Pvt Ltd, Banagalore, for extending the fabrication facility for this research work.

References

1. McWilliams, A. Nanocomposites, Nanoparticles, Nanoclays, and Nanotubes, BCC Research; 2006.
2. Osman, T. M.; Rardon, D. E.; Friedman, L. B.; Vega, L. F. JOM J Minerals, Metals Mater 2006, 58, 21.
3. Harsha, A. P.; Tewari, U. S. Polym Test 2003, 22, 403.
4. Hutchings, I. M. Tribology, CRC Press, London 1992, p 156.
5. Neale, M. J.; Gee, M. Guide to Wear Problems and Testing for Industry, William Andrew Publishing: New York, 2001.
6. Bahadur, S.; Tabor, D. Wear 1984, 98, 1.
7. Bahadur, S.; Gong, D. Wear 1992, 154, 151.
8. Bahadur, S.; Gong, D.; Anderegg, J. W. Wear 1992, 154, 207.
9. Bahadur, S.; Gong, D.; Anderegg, J. W. Wear 1993, 164, 397.
10. Suresha, B.; Ravi Kumar, B. N.; Venkataramareddy, M.; Jayaraju, T. Mater Des 2010, 31 1993.
11. Ravi Kumar, B. N.; Suresha, B.; Venkataramareddy, M. Mater Des 2009, 30, 3852.
12. Bahadur, S.; Kappor, A. Wear 1992, 155, 49.
13. Briscoe, B. J.; Tweedale, P. J. In New Materials and their Applications, Mathews, F. L.; Buskell, N.; Hodgkinson, J. M.; Morton, J., Eds. London: Elsevier, 1987; p 187.
14. Sinha, S. K.; Biswas, K. J Mater Sci 1992, 27, 3085.
15. Zum Gahr, K. Microstructure and Wear of Materials; Elsevier: Amsterdam, 1987.
16. Friedrich, K.; Karger-Kocsis, J.; Lu, Z. J Theort Appl Fract Mech 1993, 19, 1.
17. Bijwe, J.; Tewari, U. S.; Vasudevan, P. Wear 1990, 138, 61.
18. Suresha, B.; Chandramohan, G.; Sadananda Rao, P. R.; Samapathkumaran, P.; Seetharamu, S. J Reinforc Plast Compos 2007, 26, 81.
19. Palabiyik, M.; Bahadur, S. Wear 2000, 246, 149.
20. Palabiyik, M.; Bahadur, S. Wear 2002, 253, 369.
21. Stuart, B. H. Tribol Int 1998, 31, 647.
22. Biswas, S. K.; Vijayan, K. Wear 1992, 158, 193.
23. Suresha, B.; Chandramohan, G.; Siddaramaiah, S. P.; Seetharamu, S. Mater Sci Eng A 2007, 443, 285.
24. Stachowaik, G. W.; Batchelor, A. W. Engineering Tribology; Butterworth Hein Mann: Boston, 2000.
25. Bijwe, J.; Jhon Rajesh, J.; Jayakumar, A.; Gosh, A.; Tewari, U. S. Tribol Int 2000, 33, 697.
26. Bijwe, J.; Indumathi, J.; Jhon Rajesh, J.; Fahim, M. Wear 2001, 249, 715.
27. Friedrich, K.; Cyffka, M. Wear 1985, 103, 333.
28. Chand, N.; Naik, A. M.; Khaira, H. K. Polym Compos 2007, 28, 267.
29. Ozel, A. Sci Eng Compos Mater 2006, 13, 235.
30. Unal, H.; Findik, F. Indl Lub Tribol 2008, 60, 195.
31. Hasmi, S. A. R.; Chand, N.; Kitano, T. Indian J Eng Mater Sci 1998, 5, 312.

32. Bahadur, S.; Gong, D. Wear 1993, 162–164, 397.
33. Zhao, Q.; Bahadur, S. Wear 1998, 217, 62.
34. Zhao, Q.; Bahadur, S. Wear 1999, 225–229, 660.
35. Chand, N.; Pandey, A. Met Mater Process 2000, 12, 91.
36. Wang, H. G.; Qi Jian, L.; Li Pan, B.; Zhang, J. Y.; Yang, S. R. Polym Eng Sci 2007, 45, 738.
37. Srinath, G.; Gnanmoorthy, R. J Mater Sci 2005, 40, 2897.
38. Dasari, A.; Yu, Z. Z.; Mai, Y. Compos Sci Technol 2005, 65, 2314.
39. LeBaron, P. C.; Wang, Z.; Pinnavaia, T. J Appl Clay Sci 1999, 15, 11.
40. Alexandre, M.; Dubois, P. Mater Sci Eng R Rep 2000, 28, 1.
41. Okada, A.; Usuki, A. Macromol Mater Eng 2006, 291, 1449.
42. Park, H. M.; Li, X.; Jin, C. Z.; Park, C. Y.; Cho, W. J.; Ha, C. S. Macromol Mater Eng 2002, 287, 553.
43. Wilhelm, H. M.; Sierakowski, M. R.; Souza, G. P.; Wypych, F. Carbohydr Polym 2003, 52, 101.
44. Huang, M. F.; Yu, J. G.; Ma, X. F. Polymer 2004, 45, 7017.
45. Chen, B.; Evans, J. R. G. Carbohydr Polym 2005, 61, 455.
46. Ma, X.; Yu, J.; Wang, N. Macromol Mater Eng 2007, 292, 723.
47. Yu, L.; Dean, K.; Dong Yang, W. Compos Sci Technol 2007, 67, 413.
48. Chow, W. S.; Ishak, Z. A.; Kocsis, J. K.; Apostolov, A. A.; Ishiaku, U. S. Polymer 2003, 44, 7427.
49. Chow, W. S.; Ishak, Z. A.; Kocsis, J. K.; Apostolov, A. A.; Ishiaku, U. S. J Appl Polym Sci 2003, 91, 175.
50. Wahit, M. U.; Hassan, A.; Rahmat, A. R.; Lim, J. W.; Mohd Ishak, Z. A. J Reinforc Plast C 2006, 25, 933.
51. Zum Gahr, K. H. Tribol Int 1998, 31, 587.
52. Lancaster, J. K. Wear 1969, 14, 233.
53. Lancaster, J. K. Polymer Science: A Materials Science Handbook; North Holland: Amsterdam, 1972.
54. Ratner, S. N.; Farberova, I. I.; Radynekevich, O. V.; Lure, E. G. Sov Plast 1964, 7, 37.